# ChemComm

## COMMUNICATION

Check for updates

# Nitrous oxide activation by picoline-derived Ni–CNP hydrides†

José Bermejo,‡ Isabel Ortega-Lepe,‡ Laura L. Santos, Nuria Rendón, ![ORCID]
Joaquín López-Serrano, ![ORCID] Eleuterio Álvarez ![ORCID] and Andrés Suárez ![ORCID] *

Oxygen atom transfer (OAT) from $N_2O$ to the Ni–H bond of proton-responsive picoline-derived CNP nickel complexes has been investigated both experimentally and theoretically. These Ni–CNP complexes efficiently catalyse the reduction of $N_2O$ with pinacolborane (HBpin) under mild conditions.

Nitrous oxide ($N_2O$) is an important contributor to the global climate change due to its high greenhouse impact and ozone-depleting properties.[1,2] The increasing concentrations of $N_2O$ in the Earth's atmosphere have been chiefly attributed to anthropogenic sources associated with the use of nitrogen-based fertilizers, combustion of biomass and fossil fuels, and the production of industrial chemicals.[3] While thermodynamically very favourable, $N_2O$ degradation to $N_2$ and $O_2$ is associated with high kinetic barriers, which explains its average long life (118 years) in the atmosphere.[4] The known ability of transition metal complexes to react with small molecules, including $CO_2$, CO or $H_2$, make them interesting alternatives for $N_2O$ activation and subsequent transformation. However, the reactivity of transition metal complexes towards $N_2O$ is critically hampered by its weak σ-donor and π-acceptor properties as a ligand.[5] Interestingly, a favourable pathway for $N_2O$ activation by transition metal complexes involves the nucleophilic attack of a metal-bound hydride to the terminal nitrogen of $N_2O$, thus generating an O-bound oxyldiazene intermediate (M–ONNH). Subsequent nitrogen extrusion from this derivative produces a hydroxy complex (M–OH), this process representing an overall oxygen atom transfer (OAT) to the complex's M–H bond.[6–11] Moreover, the reaction of the hydroxyl derivative with common reductants, such as $H_2$,[6,7] alcohols,[8] CO[9] or silanes,[7,10] might lead to the regeneration of the M–H bond, either in a stoichiometric or catalytic process.

With the exception of a hafnium hydride complex,[11] metal systems examined for the OAT from $N_2O$ to M–H bonds are based on electron-rich precious metals (Rh, Ru, Os, Ir).[6–10] In recent years, efficient catalytic systems incorporating Earth-abundant first-row transition metals are in great demand due to their lower economic and environmental costs. As a result of being less hydridic, hydride complexes of first-row late transition metals often lack the high reactivity usually associated with their precious metal counterparts.[12] Nickel hydride pincer complexes have been found to be active catalysts in a plethora of reduction reactions,[13,14] and have been profusely investigated in the activation of $CO_2$,[15–17] an isoelectronic molecule to $N_2O$. Moreover, nickel derivatives have been shown to activate $N_2O$ by different modes.[18] Herein, we report on the reactivity of Ni–H pincer complexes based on a picoline-derived CNP (C = N-heterocyclic carbene, P = phosphine) ligand towards $N_2O$, including the OAT from $N_2O$ to the metal-hydride bond and the catalytic activity of these complexes in the reduction of $N_2O$ with pinacolborane (HBpin).
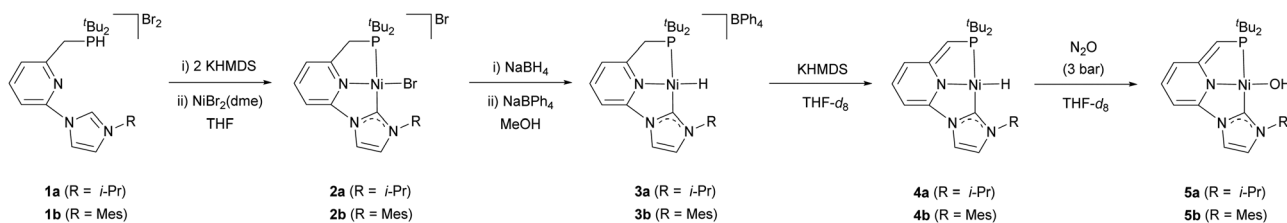
The reaction of the carbene ligand precursors **1a–b**[19] with KHMDS (potassium bis(trimethylsilyl)amide), followed by addition of $NiBr_2$(dme) (dme = 1,2-dimethoxyethane), afforded the isolation of the bromide complexes **2a–b** in good yields (83–87%) (Scheme 1). These derivatives were characterised by NMR spectroscopy and elemental analysis. Aiming to access Ni hydride pincer derivatives, the reaction of the bromide complexes **2a–b** with $NaBH_4$ was targeted. Upon anion exchange using $NaBPh_4$, the cationic hydride complexes **3a–b** were isolated with yields of 68 and 74%, respectively. These derivatives were analytical and spectroscopically characterised. For instance, the hydride region of the $^1H$ NMR spectrum of **3a** exhibits a doublet at −18.0 ppm with a coupling constant of $^2J_{HP} = 72$ Hz. The IR spectra of **3a** and **3b** include a band at 1901 and 1888 cm$^{-1}$, respectively, attributable to the stretching of the Ni–H bond. Moreover, the proposed structure of complex **3a** was further confirmed in the solid state by single crystal X-ray diffraction analysis (Fig. 1a). This complex shows a square planar coordination geometry (Σ(Ni) = 359.9°), with the pincer ligand adopting the expected $\kappa^3$-(P,N,C) coordination mode (C–Ni–P angle: 170.3°).

*Instituto de Investigaciones Químicas (IIQ) and Centro de Innovación en Química Avanzada (ORFEO-CINQA), CSIC-Universidad de Sevilla, Avda. Américo Vespucio 49, 41092, Sevilla, Spain. E-mail: andres.suarez@iiq.csic.es*

Scheme 1 Synthesis of the Ni complexes **2a–b**, **3a–b**, **4a–b** and **5a–b**.

As result of the expected acidity of the methylene hydrogens of the CNP ligand,[20] treatment of complexes **3a–b** with a strong base, such as KHMDS, in THF-$d_8$ produced the instantaneous colour change of the initially pale yellow solutions to dark red. The clean formation of the new species **4a–b**, deprotonated at the pincer methylene bridge, was evidenced by $^1H$ and $^{13}C\{^1H\}$ NMR spectroscopies. Attempted isolation of complexes **4a–b** only led to significant decomposition, likely due to a poor steric stabilization,[14] and consequently they were characterised spectroscopically in solution. In the $^1H$ NMR spectrum of **4a**, deprotonation of the methylene arm of the pincer was evidenced by the presence of a singlet appearing at 3.26 ppm, corresponding to the =CHP methyne bridge, and the up-field shift of the resonances of the dearomatized pincer central $N$-containing ring that appear between 6.41 and 5.34 ppm. In addition, a doublet resonance appearing at *ca.* −17.5 ppm ($^2J_{HP}$ = 67 Hz) in the hydride region was detected in the same experiment, which is attributable to the Ni–H hydrogen. Moreover, the stretching mode of the Ni–H bond produces in the IR spectra of **4a–b** absorption bands at lower wavelengths than in their protonated counterparts **3a–b** (1841 and 1857 cm$^{-1}$ for **4a** and **4b**, respectively), in agreement with the expected larger *trans* influence of the anionic amide central donor group of the pincer in comparison to a neutral pyridine donor.

Next, having access to the Ni hydride complexes **3** and **4**, we examined their reactions with $N_2O$. Pressurisation with $N_2O$ (3 bar) of solutions of complexes **3a–b** in THF-$d_8$ did not produced observable changes in their NMR spectra. Conversely, complexes **4a–b**, formed *in situ* by the reaction of **3a–b** with KHMDS, gradually react with $N_2O$ (3 bar) (reaction half-life of **4b**: 36 h at r.t. and 5.5 h at 55 °C) (Scheme 1). The $^1H$ NMR spectrum of the resulting hydroxy derivative **5a** includes a doublet signal attributable to the hydroxo moiety appearing at −3.85 ppm with a P–H coupling constant of $^3J_{HP}$ = 7.4 Hz; meanwhile, significant changes in the deprotonated CNP* pincer ligand were not observed. Similar spectroscopic data were obtained for complex **5b**. Analysis by X-ray diffraction of a single crystal of **5b** revealed a square-planar coordination geometry ($\Sigma(Ni)$ = 360.1°, C–Ni–P angle: 166.65(7)°), with quite similar metric parameters to the Ni-pincer framework of complex **3a** (Fig. 1b). The Ni atom in **5b** resides in a distorted square-planar environment with the hydroxyl oxygen displaced 0.17 Å out of the least-square plane defined by the P1, C1, N3 and Ni atoms. Finally, the Ni–O bond length, 1.8272(18) Å, lies at the lowest extreme of the range observed for related nickel square-planar hydroxo complexes based on anionic pincer ligands (Ni–O distances: 1.83–1.93 Å).[21] It is remarkable that, to our knowledge, this is the first example of an OAT from $N_2O$ to a base metal hydride complex.

To attain further insight into the observed dissimilar reactivity of complexes **3** and **4** towards $N_2O$, the mechanism of the $N_2O$ oxygen atom transfer to the Ni–H bonds of **3a** and **4a** was investigated by performing DFT calculations (B3LYP-D3/def2TZVP) (Fig. 2). In the case of **3a**, initial outer-sphere transfer of the hydrido ligand to the terminal nitrogen atom of $N_2O$ leads to the endergonic formation of intermediate **A**, with an associated barrier $TS_{(3a\rightarrow A)}$ of 29.2 kcal mol$^{-1}$.[22] Subsequent $N_2$ release from **A** to yield the corresponding hydroxo complex **B** was found to be largely exergonic, having a relatively high energy barrier of 27.8 kcal mol$^{-1}$. Interestingly, in the case of **4a**, the transition state $TS_{(4a\rightarrow A^*)}$ associated to the transfer of the Ni–H hydride to $N_2O$ has an energy ($\Delta G^{\ddagger}$) of 26.0 kcal mol$^{-1}$, and leads to the formation of **A\*** with an energy return of 4.0 kcal mol$^{-1}$. The lower barrier for the hydride transfer to $N_2O$ for **4a** and the thermodynamically favourable formation of **A\*** resemble reported results regarding the insertion of $CO_2$ into Ni–H bonds of square-planar pincer nickel complexes.[16,17] These studies have shown lower energy barriers and higher stability of the insertion products as the ligand *trans* to the hydride becomes a stronger donor. In our case, the different behaviour of the hydrides **3** and **4** towards $N_2O$ can be attributed to the expected larger *trans* influence of the deprotonated pincer ligand, which produces a weakening of the Ni–H bond and increases the nucleophilic character of the hydride ligand.[16,17] In fact, the calculated Ni–H distances and NBO (natural bond orbital) charges on the hydride for **3a** and **4a** are in good agreement with a less strong Ni–H bond and a higher nucleophilicity of the Ni–H group in the case of **4a**. The Ni–H bond is slightly longer for **4a** [$d$(Ni–H) = 1.48 Å (**3a**), 1.51 Å (**4a**)]; whereas the hydride ligand bears a larger negative charge [NBO charges on the Ni: 0.41 (**3a**) and 0.42 (**4a**); NBO charges on the hydride: −0.24 (**3a**), −0.31 (**4a**)].
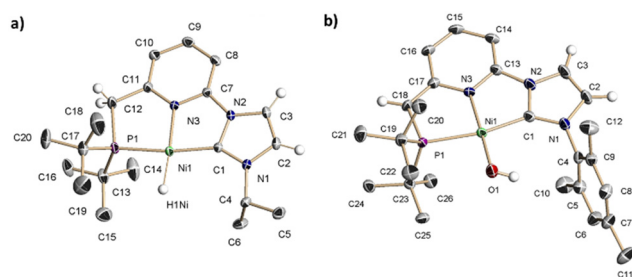


Fig. 1 ORTEP drawings at 30% ellipsoid probability of: (a) the cationic fragment of complex **3a**, and (b) complex **5b**. Most hydrogen atoms have been omitted for the sake of clarity. See ESI† for selected bond lengths and angles.
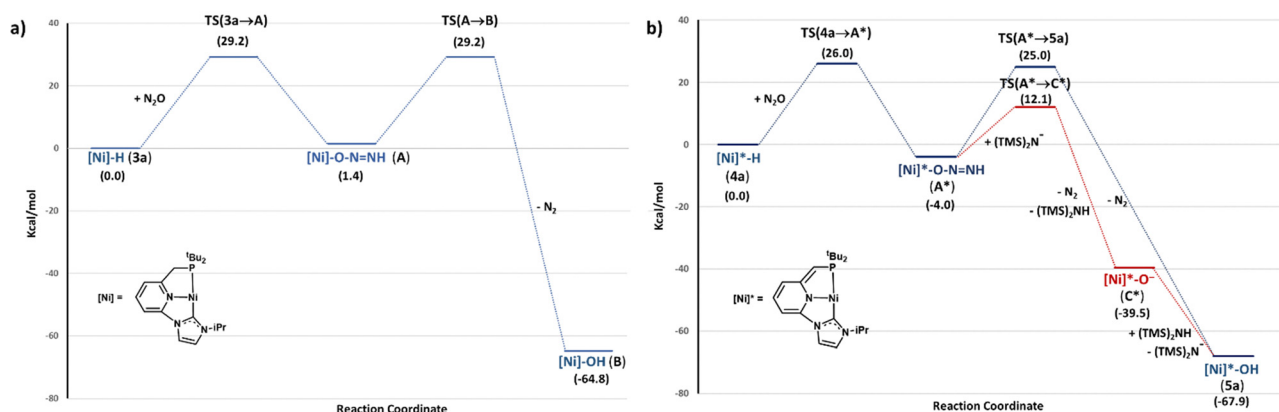
**Fig. 2** DFT calculated free energy ($\Delta G$ in THF, kcal mol$^{-1}$) profile of the N$_2$O insertion into the Ni–H bond of complexes **3a** (a) and **4a** (b).

N$_2$ extrusion from **A\*** to form the corresponding hydroxo derivative **5a** was found to be highly exergonic, having an energy barrier of 29.0 kcal mol$^{-1}$. However, since complex **4a** is generated *in situ* from **3a** in the presence of a slight excess of KHMDS, the participation of the base in the N$_2$ release step was also investigated. Deprotonation of the Ni–ONNH moiety yields the unusual species **C\*** through a transition state located at 16.1 kcal mol$^{-1}$. This intermediate can be readily protonated by (Me$_3$Si)$_2$NH leading to the hydroxo complex **5a**. This last step is exergonic by 28.4 kcal mol$^{-1}$ from **C\***, and takes place without energy barrier, as indicated by relaxed potential energy (PES) scans (see ESI†). The overall energy return for the formation of **5a** and N$_2$ from **4a** and N$_2$O is 67.9 kcal mol$^{-1}$.

Next, the catalytic performance of the Ni(II) hydride derivatives in the reduction of N$_2$O using HBpin was examined (Table 1).[23] Whilst no reaction was observed in the absence of the Ni–CNP catalysts, HBpin was fully consumed using 2.0 mol% of the cationic complexes **3a–b**, leading to the formation of pinBOH and (pinB)$_2$O, in a 2:8 ratio (entries 1 and 2); moreover, generation of N$_2$ and H$_2$ was detected, although it could not be quantified (see ESI† for details). By employing *in situ* formed complexes **4a** and **4b**, somewhat faster reactions using lower catalyst loadings (0.5 mol%) than for the corresponding complexes **3** were observed (entries 3 and 4). Finally, THF-$d_8$ solutions of complex **5b**, formed *in situ*, were also found to catalyse the reduction of N$_2$O with HBpin (entry 5).

**Table 1** N$_2$O reduction with HBpin catalysed by Ni complexes **3** and **4**[a]

| Entry | Cat. | Cat. loading [mol%] | Conv. [%] (time, [h]) | pinBOH:(pinB)$_2$O ratio |
|-------|------|---------------------|------------------------|--------------------------|
| 1 | **3a** | 2.0 | >99 (6.5) | 2:8 |
| 2 | **3b** | 2.0 | >99 (2.0) | 2:8 |
| 3 | **4a** | 0.5 | >99 (3.0) | 1:9 |
| 4 | **4b** | 0.5 | >99 (2.0) | 2:8 |
| 5 | **5b** | 2.0 | >99 (2.0) | 2:8 |

[a] Reaction conditions, unless otherwise noted: 2 bar N$_2$O, r.t., THF-$d_8$, [HBpin] = 0.4 M. Complexes **4a–b** were formed *in situ* from **3a–b** with KHMDS. Complex **5b** was formed *in situ* from **3b** and KHMDS under N$_2$O pressure. Conversion and selectivity were determined by $^1$H and $^{11}$B{$^1$H} NMR spectroscopies using mesitylene as internal standard. N$_2$ and H$_2$ formation were detected by GC-MS analysis of the headspace gas and $^1$H NMR spectroscopy, respectively (see ESI).

The observed fast kinetics for the catalytic reaction are at odds with the relatively slow N$_2$O insertion in complexes **4** and the lack of reactivity of derivatives **3**. In an attempt to obtain further information, a series of control experiments were performed. First, no reaction was observed by NMR spectroscopy between HBpin (ca. 4 equiv.) and the hydride complexes **3** and **4** in the temperature range between −60 °C and 55 °C.[24] Moreover, a solution of the *in situ* formed complex **5b** in THF-$d_8$ was treated with HBpin (0.9 equiv.) at −65 °C. After approximately 0.25 h, 82% conversion of **5b** to a mixture of the hydride derivatives **3b** and **4b** (5:1 ratio) was observed, demonstrating that Ni–H bond regeneration from **5** is facile with HBpin. In the $^{11}$B{$^1$H} NMR spectrum of this experiment, a new broad signal was observed at 4.5 ppm. Unfortunately, attempts to isolate and characterise this boron species were unsuccessful. The presence of borane Lewis acids has been shown to impact on both the reaction kinetics and product distribution in the CO$_2$ hydroboration,[25] and has been found to play a role in the CO$_2$ activation by Ni-PBP hydride complexes. Therefore, we hypothesise that Lewis acid borane species might catalyse or co-catalyse the hydroboration of N$_2$O in the presence of complexes **3** and **4**.[26] In fact, complete catalyst inhibition was observed when the reaction catalysed by **3b** was performed in the presence of 20 mol% Et$_3$N, acting as a Lewis acid scavenger.[27]

To conclude, the OAT from N$_2$O to hydride Ni complexes based on CNP ligands has been found to be dependent on the *trans* influence of the pincer. Thus, the reactivity of complexes **3a–b** towards N$_2$O is triggered by a strong base (KHMDS), leading to the formation of the deprotonated Ni–CNP\* species **4a–b**, which are capable of performing N$_2$O activation. Moreover, the use of a strong base promotes the N$_2$ release from the Ni–ONNH intermediate resulting from the N$_2$O insertion into the Ni–H bond. Finally, both complexes **3** and **4** catalyse the reduction of N$_2$O with HBpin, in a process that is proposed to be catalysed or co-catalysed by the presence of boron Lewis acids generated under catalytic conditions.

## Conflicts of interest

There are no conflicts to declare.

## Notes and references

1 J. Hansen and M. Sato, *Proc. Natl. Acad. Sci. U. S. A.*, 2004, **101**, 16109; S. A. Montzka, E. J. Dlugokencky and J. H. Butler, *Nature*, 2011, **476**, 43.
2 M. J. Prather, *Science*, 1998, **279**, 1339; A. R. Ravishankara, J. S. Daniel and R. W. Portmann, *Science*, 2009, **326**, 123.
3 E. A. Davidson and D. Kanter, *Environ. Res. Lett.*, 2014, **9**, 105012.
4 S. I. Gorelsky, S. Ghosh and E. I. Solomon, *J. Am. Chem. Soc.*, 2006, **128**, 278; S. Javoy, R. Mevel and C. E. Paillard, *Int. J. Chem. Kinet.*, 2009, **41**, 357.
5 W. B. Tolman, *Angew. Chem., Int. Ed.*, 2010, **49**, 1018.
6 A. W. Kaplan and R. G. Bergman, *Organometallics*, 1997, **16**, 1106; A. W. Kaplan and R. G. Bergman, *Organometallics*, 1998, **17**, 5072; J.-H. Lee, M. Pink, J. Tomaszewski, H. Fan and K. G. Caulton, *J. Am. Chem. Soc.*, 2007, **129**, 8706; L. E. Doyle, W. E. Piers and J. Borau-Garcia, *J. Am. Chem. Soc.*, 2015, **137**, 2187; J. D. Smith, E. Chih, W. E. Piers and D. M. Spasyuk, *Polyhedron*, 2018, **155**, 281; P. Jurt, A. S. Abels, J. J. Gamboa-Carballo, I. Fernández, G. Le Corre, M. Aebli, M. G. Baker, F. Eiler, F. Müller, M. Wörle, R. Verel, S. Gauthier, M. Trincado, T. L. Gianetti and H. Grützmacher, *Angew. Chem., Int. Ed.*, 2021, **60**, 25372; I. Ortega-Lepe, P. Sánchez, L. L. Santos, P. Lara, N. Rendón, J. López-Serrano, V. Salazar-Pereda, E. Álvarez, M. Paneque and A. Suárez, *Inorg. Chem.*, 2022, **61**, 18590.
7 R. Zeng, M. Feller, Y. Ben-David and D. Milstein, *J. Am. Chem. Soc.*, 2017, **139**, 5720.
8 T. L. Gianetti, S. P. Annen, G. Santiso-Quinones, M. Reiher, M. Driess and H. Grützmacher, *Angew. Chem., Int. Ed.*, 2016, **55**, 1854; J. Bösken, R. E. Rodríguez-Lugo, S. Nappen, M. Trincado and H. Grützmacher, *Chem. – Eur. J.*, 2023, **29**, e202203632.
9 R. Zeng, M. Feller, Y. Diskin-Posner, L. J. W. Shimon, Y. Ben-David and D. Milstein, *J. Am. Chem. Soc.*, 2018, **140**, 7061.
10 P. Molinillo, B. Lacroix, F. Vattier, N. Rendón, A. Suárez and P. Lara, *Chem. Commun.*, 2022, **58**, 7176.
11 G. A. Vaughan, P. B. Rupert and G. L. Hillhouse, *J. Am. Chem. Soc.*, 1987, **109**, 5538.
12 E. S. Wiedner, M. B. Chambers, C. L. Pitman, R. M. Bullock, A. J. M. Miller and A. M. Appel, *Chem. Rev.*, 2016, **116**, 8655.
13 V. Arora, H. Narjinari, P. G. Nandia and A. Kumar, *Dalton Trans.*, 2021, **50**, 3394.
14 N. A. Eberhardt and H. Guan, *Chem. Rev.*, 2016, **116**, 8373.
15 T. J. Schmeier, N. Hazari, C. D. Incarvito and J. A. Raskatov, *Chem. Commun.*, 2011, **47**, 1824; J. E. Heimann, W. H. Bernskoetter, J. A. Guthrie, N. Hazari and J. M. Mayer, *Organometallics*, 2018, **37**, 3649; C. Yoo, J. Kim and Y. Lee, *Organometallics*, 2013, **32**, 7195; K. J. Jonasson and O. F. Wendt, *Chem. – Eur. J.*, 2014, **20**, 11894;

L. J. Murphy, H. Hollenhorst, R. McDonald, M. Ferguson, M. D. Lumsden and L. Turculet, *Organometallics*, 2017, **36**, 3709.
16 H.-W. Suh, T. J. Schmeier, N. Hazari, R. A. Kemp and M. K. Takase, *Organometallics*, 2012, **31**, 8225.
17 P. Ríos, N. Curado, J. López-Serrano and A. Rodríguez, *Chem. Commun.*, 2016, **52**, 2114; P. Ríos, A. Rodríguez and J. López-Serrano, *ACS Catal.*, 2016, **6**, 5715; J. E. Heimann, W. H. Bernskoetter, N. Hazari and J. M. Mayer, *Chem. Sci.*, 2018, **9**, 6629; T. J. Schmeier, A. Nova, N. Hazari and F. Maseras, *Chem. – Eur. J.*, 2012, **18**, 6915.
18 T. Yamada, K. Suzuki, K. Hashimoto and T. Ikeno, *Chem. Lett.*, 1999, 1043; P. T. Matsunaga and G. L. Hillhouse, *J. Am. Chem. Soc.*, 1993, **115**, 2075; N. D. Harrold, R. Waterman, G. L. Hillhouse and T. R. Cundari, *J. Am. Chem. Soc.*, 2009, **131**, 12872; B. Horn, C. Limberg, C. Herwig, M. Feist and S. Mebs, *Chem. Commun.*, 2012, **48**, 8243; F. Le Vaillant, A. Mateos Calbet, S. González-Pelayo, E. J. Reijerse, S. Ni, J. Busch and J. Cornella, *Nature*, 2022, **604**, 677; J. Gwak, S. Ahn, M.-H. Baik and Y. Lee, *Chem. Sci.*, 2019, **10**, 4767.
19 T. Simler, A. A. Danopoulos and P. Braunstein, *Chem. Commun.*, 2015, **51**, 10699.
20 J. I. van der Vlugt, M. Lutz, E. A. Pidko, D. Vogt and A. L. Spek, *Dalton Trans.*, 2009, 1016; D. Oren, Y. Diskin-Posner, L. Avram, M. Feller and D. Milstein, *Organometallics*, 2018, **37**, 2217.
21 T. J. Schmeier, A. Nova, N. Hazari and F. Maseras, *Chem. – Eur. J.*, 2012, **18**, 6915; D. Adhikari, S. Mossin, F. Basuli, B. R. Dible, M. Chipara, H. Fan, J. C. Huffman, K. Meyer and D. J. Mindiola, *Inorg. Chem.*, 2008, **47**, 10479; D. V. Gutsulyak, W. E. Piers, J. Borau-Garcia and M. Parvez, *J. Am. Chem. Soc.*, 2013, **135**, 11776; J. Cámpora, P. Palma, D. del Río and E. Álvarez, *Organometallics*, 2004, **23**, 1652; A. Castonguay, A. L. Beauchamp and D. Zargarian, *Inorg. Chem.*, 2009, **48**, 3177; C. Yao, P. Chakraborty, E. Aresu, H. Li, C. Guan, C. Zhou, L.-C. Liang and K.-W. Huang, *Dalton Trans.*, 2018, **47**, 16057; K. J. Jonasson, A. H. Mousa and O. F. Wendt, *Polyhedron*, 2018, **143**, 132; N. H. Anderson, J. M. Boncella and A. M. Tondreau, *Organometallics*, 2018, **37**, 4675.
22 H. Yu, G. Jia and Z. Lin, *Organometallics*, 2008, **27**, 3825; J. A. Luque-Urrutia and A. Poater, *Inorg. Chem.*, 2017, **56**, 14383; L. Yao, L. Huang, K. Guo, G. Ren, Z. Wu, Q. Lei, W. Fang and H. Xie, *Comput. Theor. Chem.*, 2018, **1128**, 48; H. Xie, C. Liu, Y. Yuan, T. Zhou, T. Fan, Q. Lei and W. Fang, *Dalton Trans.*, 2016, **45**, 1152; S. Escayola, M. Solà and A. Poater, *Inorg. Chem.*, 2020, **59**, 9374; H. Xie, Y. Zhang, C. Xiang, Y. Li, T. Fan, Q. Lei and W. Fang, *Dalton Trans.*, 2018, **47**, 15324; G. Liang, M. Zhang and C. E. Webster, *Inorganics*, 2022, **10**, 69; H. Xie, Y. Li, L. Huang, F. Nong, G. Ren, T. Fan, Q. Lei and W. Fang, *Dalton Trans.*, 2016, **45**, 16485.
23 Y. Pang, M. Leutzsch, N. Nöthling and J. Cornella, *J. Am. Chem. Soc.*, 2020, **142**, 19473; X. Chen, H. Wang, S. Du, M. Driess and Z. Mo, *Angew. Chem., Int. Ed.*, 2022, **61**, e202114598.
24 D. Adhikari, J. C. Huffman and D. J. Mindiola, *Chem. Commun.*, 2007, 4489; A. Rossin, M. Peruzzini and F. Zanobini, *Dalton Trans.*, 2011, **40**, 4447; S. Chakraborty, J. Zhang, Y. J. Patel, J. A. Krause and H. Guan, *Inorg. Chem.*, 2013, **52**, 37.
25 M. R. Espinosa, D. J. Charboneau, A. Garcia de Oliveira and N. Hazari, *ACS Catal.*, 2019, **9**, 301.
26 S. J. Geier, C. M. Vogels, J. A. Melanson and S. A. Westcott, *Chem. Soc. Rev.*, 2022, **51**, 8877.
27 A. D. Bage, K. Nicholson, T. A. Hunt, T. Langer and S. P. Thomas, *ACS Catal.*, 2020, **10**, 13479.